

The vulnerability of road networks under area-covering disruptions

Erik Jenelius
Lars-Göran Mattsson

Div. of Transport and Location Analysis
Dept. of Transport and Economics
Royal Institute of Technology (KTH), Stockholm, Sweden

22 October 2008

Abstract

We present a method to analyse the vulnerability of road networks under area-covering disruptions. Since various kinds of real-world events such as snow storms and floods can cause such spatially extended disruptions, the analysis method is an important complement to the existing studies of single link failures. The approach is based on covering the study area with grids of equally shaped and sized cells, where each cell represents the extent of a disrupting event. We apply the method to the Swedish road network. The case study shows that the factors determining where an area-covering disruption will have the worst consequences are quite different from those of a single link failure. In the latter case, the flow on the link and the availability of alternative routes, i.e. the redundancy in the network, determines the consequences. For area-covering disruptions, the network redundancy has a much smaller impact, since nearby potential alternative links are often also disabled. It is the travel demand within, into and out from the affected area that largely determines the magnitude of the consequences.

1. Introduction

The road transport system is one of the fundamentals of modern society. Its ability to connect spatially separated locations is vital for the accessibility and welfare of people and the economic efficiency of businesses. Even if the fossil fuel car is gradually replaced by more environmentally sustainable means of transport, the road network is likely to remain a central component of the transport infrastructure in the foreseeable future.

Since the road network is such a vital part of society, disruptions in the network, when they occur, often have severe consequences. In the worst cases, such disturbances can impair the ability for people to receive emergency medical care and other societal services. Beside the threat to life and health, disruptions can cause substantial economic and social strains. For people, this includes impaired abilities to commute, to drop off and pick up children from daycare and school, to do the shopping, etc. For companies, the impacts can include delayed deliveries and supplies, increased freight costs, delayed or cancelled business meetings, etc.

Many types of events can cause this kind of network degradations. Some events, such as traffic accidents, originate within the transport system, while others, such as floods, land slides, snow storms and earthquakes, are external strains imposed on the system. Some events are concentrated in space and affect only a single link in the network, while others (typically of external origin) extend across a larger area, disrupting several links.

There is a growing literature concerned with vulnerability analysis of transport networks. So far, most attention has been devoted to developing metrics to capture the consequences of network degradation, and on identifying the most important (or critical) links, i.e. links that if disabled one at a time would cause the most severe consequences (Murray-Tuite and Mahmassani, 2004; Jenelius et al., 2006; Scott et al., 2006; Sohn, 2006; Taylor et al., 2006; Chen et al., 2007; Qiang and Nagurney, 2008; Jenelius, E., 2008b). The focus of the present paper, in contrast, is on systematic analysis of more spatially extended, area-covering network degradations. As far as the authors know, no such analysis has been presented previously.

The impacts of degradations of extended areas in the transport system may be quite different from single link failures. In a dense road network a single link failure may result in only short detours for the travellers, whereas in a sparse network a link failure may cause very long detours and delays. If an extended area is disrupted, in contrast, many links in the dense network may be disabled and many travellers affected, whereas only a few links may be disabled in the sparse network. Thus, it can be expected that redundancy in the network, which is of great importance under single link failures, will be of much less benefit in the case of area-covering disruptions. This aspect of vulnerability is likely missed if only single link failures are considered.

In this paper we present a method for systematically studying the geographic variations of road network vulnerability under area-covering disruptions. Since many kind of events, for instance snow storms, floods and forest fires, can have such effects, this kind of analysis is an important complement to the analysis of single link failures. The approach avoids the potential combinatorial problems associated with multiple link failures and is not biased regarding which parts of the transport system are covered by the disruptions.

With our approach, the transport network representation is covered by a grid of uniformly shaped and sized cells, where each cell represents the spatial extent of a disrupting event. For each cell all links intersecting it are identified. The consequences of disabling these links simultaneously, in terms of increased travel time and unsatisfied demand for the users, are calculated. We can then study the impacts of a disrupting event of this magnitude depending on its spatial location. We can also identify geographic regions that are particularly exposed to an event of this kind. Multiple grids of the same cell size, evenly displaced from each other, can be used to increase the accuracy of the analysis.

The structure of the paper is as follows. The methodology is described in Section 2. In Section 3 we present an application of method to the Swedish road transport network, with results given in Section 4. The paper ends with conclusions and a discussion of the strengths and weaknesses of the method in Section 5.

2. Methodology

2.1 Grid-based vulnerability analysis

When extending road network vulnerability analysis from single link failures to area-covering failures, the set of scenarios to consider must be chosen in a systematic way. In reality, an event such as a snow storm may cause some links in the affected area to be completely blocked, others to have their capacities reduced, and still others to be virtually unaffected. For large networks, the number of possible combinations of link states makes it unfeasible to

consider all these combinations. Our approach to reduce the number of scenarios is to define a precise spatial location and extent for the disrupting event. Links within or intersecting this area are completely closed, while links outside the area are completely unaffected.

Furthermore, the locations of the disrupting events should not be biased towards certain regions if we are to make systematic geographical comparisons. For example, it might at first seem appropriate to approximate the disrupting event with a circular area. However, depending on how far apart we position these circles, some regions of the study area may not be covered by any circle, or some regions may be covered by more circles than others. This creates a bias in the results depending on which regions happen to be more covered. Our approach, instead, is to make a complete coverage of the study area using a grid of equally shaped and sized cells. This guarantees that a specific square inch of land is covered by one and only one event. The most circular-like cell shape that can partition a study area in such a way is the hexagon. As explained in more detail in Section 3, we use square cells in the case study presented in this paper.

Since the cells in a grid are non-overlapping, the results can be sensitive to how the grid is positioned over the study area. To increase the detail and accuracy of the analysis, we can superimpose multiple grids of the same size and shape and calculate the results for every cell in every grid. Figure 1 illustrates how four square grids can be displaced so that any given point in the study area is covered by four cells. A disadvantage of using non-circular areas to represent disrupting events is that the results depend on how the grid is rotated relative to the study area. However, we think that the advantages of using a covering grid outweighs this drawback.

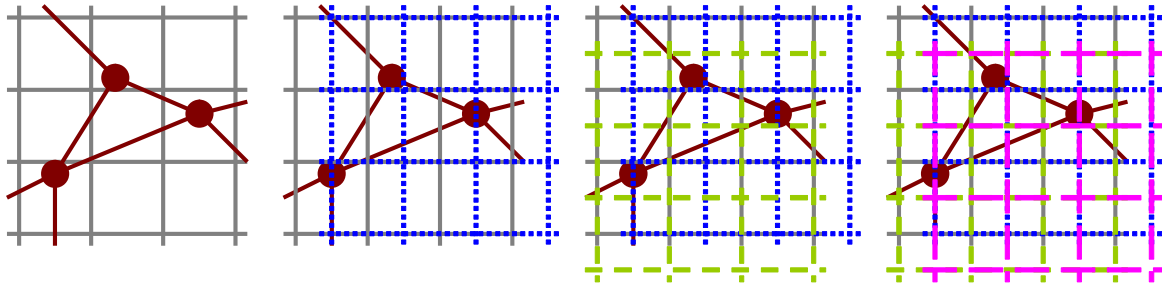


Fig. 1: Four square grids of equal size, symmetrically displaced.

2.2 Cell importance

In parallel with the concept of link importance, we can define the importance of a particular grid cell to be the total consequences for the network users of a disrupting event in the cell, closing all intersecting links. In this paper we will use increases in travel time or delays to operationalize the consequences.

Formally, let $\Delta T_{ij}^c(\tau)$ be the increase in vehicle travel time for all users travelling from zone i to zone j during a closure of all links intersecting cell c with duration τ . Then the importance of c , given τ , is the sum of $\Delta T_{ij}^c(\tau)$ over all OD relations,

$$I(c | \tau) = \sum_i \sum_{j \neq i} \Delta T_{ij}^c(\tau).$$

2.3 Regional exposure

The concept of regional exposure was introduced in Jenelius et al. (2006). Given a scenario, the exposure of a region is the consequences for the users travelling from the region if the scenario would occur. Jenelius (2008a) further divided exposure into total exposure, measured as the total increase in vehicle travel time, and user exposure, measured as the mean increase in travel time per user.

Just as importance, the exposure concept can be extended to area-covering disruptions. In this paper we will consider a worst-case scenario, where the most important cell for the region is closed. Formally, let r denote a region in the study area and let $i \in r$ mean that zone i (or its centroid) is located in region r . Given closure duration τ and a collection of grids G , the worst-case total exposure of region r is then

$$\text{TE}_{\text{wc}}(r | \tau, G) = \max_{c \in G} \sum_{i \in r} \sum_{j \neq i} \Delta T_{ij}^c(\tau).$$

Let x_{ij} denote the average travel demand (in vehicles per unit time) between zone i and j during the closure. Then the worst-case user exposure of region r is

$$\text{UE}_{\text{wc}}(r | \tau, G) = \max_{c \in G} \frac{\sum_{i \in r} \sum_{j \neq i} \Delta T_{ij}^c(\tau)}{\sum_{i \in r} \sum_{j \neq i} x_{ij} \tau}.$$

2.4 Travel time model

In the case study we use the travel time model from Jenelius (2008a,b). A benefit of the model is that it incorporates closures regardless of whether there are alternative routes available or not. For area-covering disruptions this is important, since some OD relations may have alternative routes while others may not. It is applicable to very large, mainly uncongested road networks, where computation time and memory consumption are important issues. In particular, it is assumed that the closure of a link does not affect the travel time on any other link. This approximation should be valid for most of the Swedish road network used in the case study, which is largely uncongested. In densely populated areas, however, the model can be expected to underestimate the delays caused by a closure. That being said, users who are unable to travel during the closure will not contribute to congestion, so the congestion effects may not necessarily be much worse for area-covering failures than single link failures.

During the closure of the links intersecting cell c , there may be either no or at least one alternative route from origin i to destination j . If there are no alternative routes, the best a user can do is to wait until cell c is reopened. Assuming that the travel demand is constant over time, a user wishing to depart during the closure will on average be delayed $\tau / 2$ time units. The total demand during the closure is $x_{ij} \tau$ and the total increase in vehicle travel time during this period is

$$\Delta T_{ij}^c(\tau) = \frac{x_{ij} \tau^2}{2}.$$

Since the users are unable to travel during the closure, we will refer to x_{ij} as *unsatisfied demand*.

If there are alternative routes, a user can choose to travel along the new shortest route or to wait until the links in c are reopened if this means reaching the destination faster. Let Δt_{ij}^c denote the difference in travel time between the new and the original shortest route, which we assume is known to the users. It can be shown that the total increase in vehicle travel time during the closure in any case is

$$\Delta T_{ij}^c(\tau) = \begin{cases} \frac{x_{ij}\tau^2}{2} & \text{if } \Delta t_{ij}^c \geq \tau, \\ x_{ij}\tau\left(\Delta t_{ij}^c - \frac{\tau}{2}\right) & \text{if } \Delta t_{ij}^c < \tau. \end{cases}$$

3. Case study

3.1 Specifications

We have applied the measures proposed in Section 2 to the Swedish road network. In this study we have used square cells to represent the area-covering disruptions. There were several reasons for using square, rather than hexagonal, cells. First, square grids are considerably easier to create and work with using GIS raster techniques. Second, we hope in the future to attach data to the cells in order to estimate the relative probabilities of disruptive events in different cells. It is likely that such data would be available in (square shaped) raster form.

We have used grids with three different cell sizes: $50 \times 50 \text{ km}^2$, $25 \times 25 \text{ km}^2$ and $12.5 \times 12.5 \text{ km}^2$, respectively. For the largest cell size we have used 16 grids, evenly displaced in four columns and four rows. For the two smaller cell sizes we have used four grids, symmetrically displaced in two columns and two rows. The $50 \times 50 \text{ km}^2$ grids consist of 16×32 cells each, the $25 \times 25 \text{ km}^2$ grids consist of 32×64 cells each, and the $12.5 \times 12.5 \text{ km}^2$ grids consist of 64×128 cells each. To illustrate the size of the events that we consider, Figure 2 shows a portion of the smallest grid laid over the study area.

For each grid, we have calculated the importance of every cell. For each point of the study area, the results are presented as an average over the cells from the different grids that cover the point. For the 12.5 km grid, this gives a resolution of 6.25 km , while the resolution for the two larger grid sizes becomes 12.5 km .

We have also calculated the worst-case user exposure for each county in Sweden. For each grid size, the most important cell for each county is identified across all displaced grids. For comparison, we have also calculated the worst-case user exposure to a single-link failure. In all calculations, we have assumed that the duration of the closure is 12 hours. This is a relatively short duration considering the geographic extent of the disruptions, and is intended to represent something like a snow storm, where the links can be ploughed and reopened fairly rapidly. As the results will show, the closure duration actually has a very small impact on the relative importance and exposure of different cells and counties.

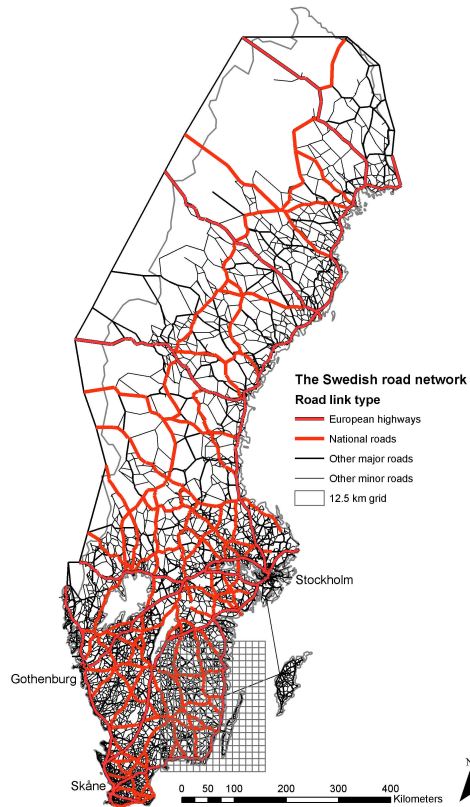


Fig. 2: The Swedish road network representation.

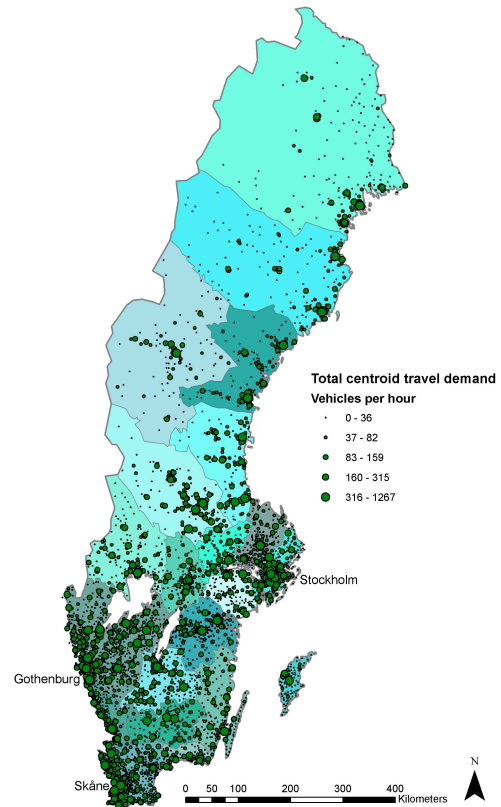


Fig. 3: Total travel demand from every centroid.

3.2 Data and computations

We have obtained the data for the Swedish road network from the Swedish national travel demand model system SAMPERS (Beser and Algers, 2001). In SAMPERS, the travel demand between different zones is calculated using nested logit choice models which have been estimated on travel surveys. The travel time of each link is calculated with user equilibrium traffic assignments in EMME/2 (using a 0.001 relative gap stop criterion), which means that initial congestion is considered in this study. The OD travel demand matrix used in our study represents the annual daily average travel demand and includes both car and truck trips.

The SAMPERS system divides Sweden into zones in which all trips begin and end, each zone comprising about 1,000 inhabitants. For computational reasons, SAMPERS has divided the Swedish transport system into five complementary regional submodels. We have obtained a detailed representation of the entire national road transport system by merging the regional submodels while retaining all interregional trips. A few links in Norway and Finland have been added to provide alternative routes and reduce border effects, but are not disabled in the vulnerability analysis. The resulting road network consists of 77,769 nodes (including 8,764 centroids) and 174,044 directed links, and represents a very fine level of detail. The representation of the Swedish road network is shown in Figure 2. In Figure 3 every centroid is shown with sizes reflecting the total travel demand originating from the centroid to all other zones.

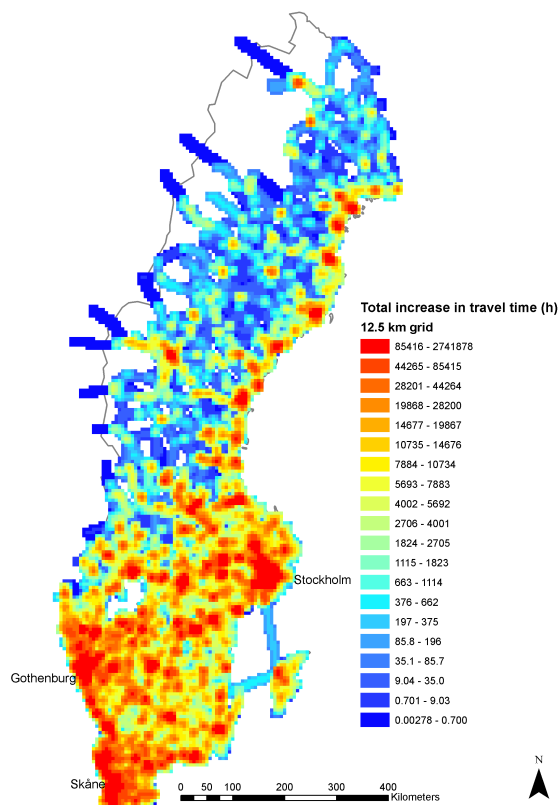


Fig. 4: Cell importance for 12.5 km grids.

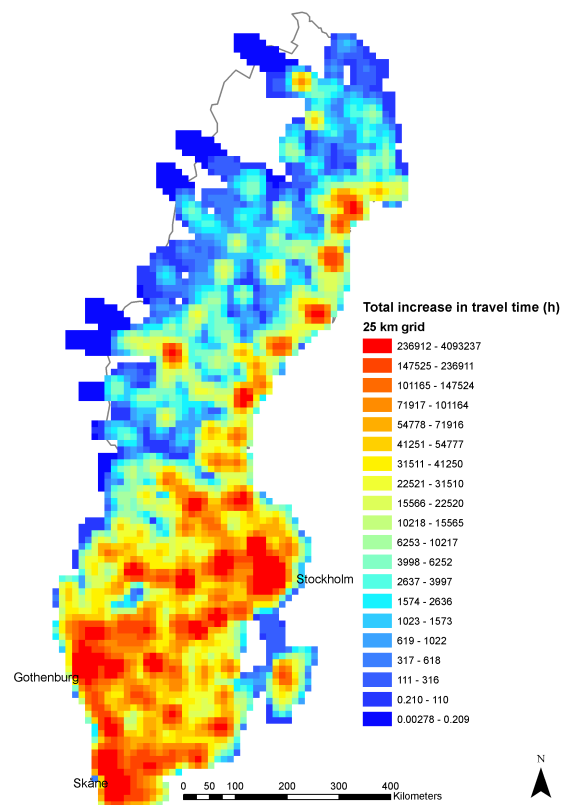


Fig. 5: Cell importance for 25 km grids.

The grids were created with a GIS, which was also used to identify all links intersecting each cell. The vulnerability calculations were performed with specially developed software written in C++/C#. Using a 2.0 GHz Pentium III 1 GB laptop, calculating the the importance of every cell and the exposure of every county for a specific grid takes about 12 hours. These reasonable computation times could not have been obtained without the assumption that link travel times are independent of link flows. For each origin i , the original travel times to all destinations are calculated using Dijkstras algorithm, implemented with approximate buckets (Zhan and Noon, 1998). To calculate the consequences of a cell closure, the shortest path tree is then either iteratively updated using a reoptimization algorithm (Buriol et al., 2004) (faster for small grid sizes), or recalculated from scratch after the links have been disabled (faster for large grid sizes).

4. Results

4.1 Cell importance

In Figures 4, 5 and 6 the importance of every cell is shown for the three different grid sizes. As explained above, each small square in the diagram represent an average over the cells from the different displaced grids that covers it. With the smallest grid size, it is possible to discern many features of the transport system and the locations of population centras, which appear as red spots on the map. As the grid size increases, the diagrams tend to reflect the population density of Sweden more than the road network. This is reasonable, since the more wide-spread the disruption, the more people should live directly within the disrupted area and be unable to travel.

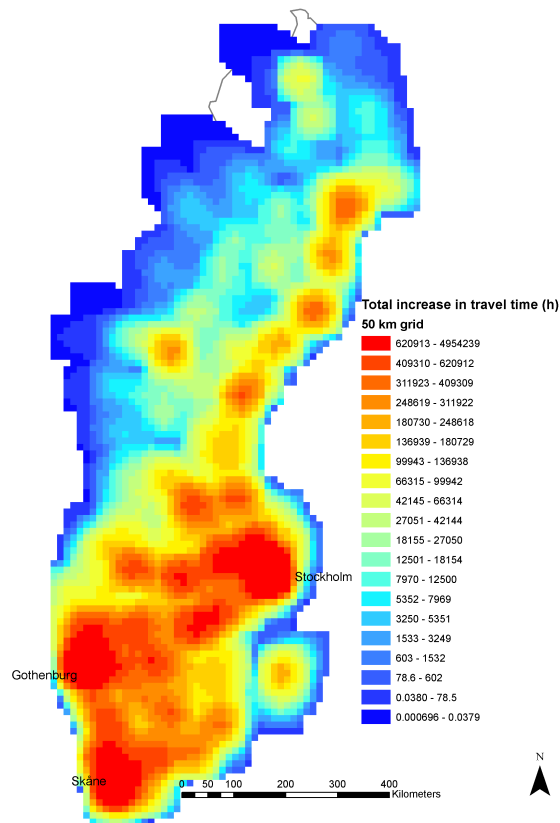


Fig. 6: Cell importance for 50 km grids.

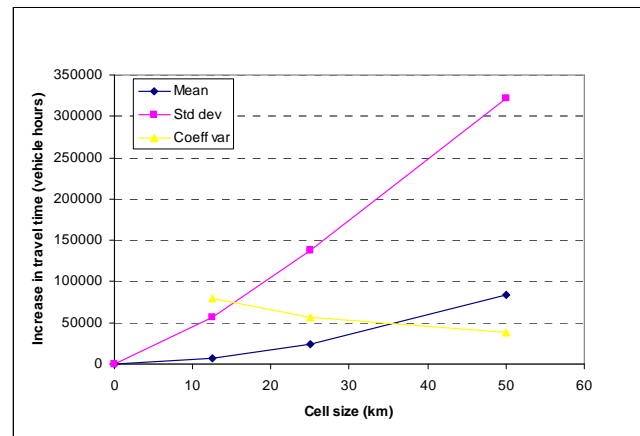


Fig. 7: The mean and standard deviation of the increase in travel time as functions of the grid size.

Figure 7 shows how the consequences of closing a cell depend on the grid size. As can be seen, the mean increase in travel time increases with the grid size, as would be expected. The increase rate is slightly less than quadratic with an estimated exponent of about 1.78. The variation between cells, as measured by the coefficient of variation (standard deviation divided by mean), decreases slightly.

The analysis shows that almost all of the increase in travel time caused by an area-covering disruption is due to users who are completely cut off and must wait until the links are reopened. For the 12.5 km grids, this unsatisfied demand constitutes 97.6 % of the total increase in travel time on average; for the 50 km grid the share is as high as 99.3 %. This implies that the closure duration has little impact on the relative importance of different cells.

4.2 Worst-case county user exposure

Figure 8 shows the worst-case user exposure for each county in Sweden and the 12.5 km grids, i.e. the mean increase in travel time per user when the most important 12.5 km cell for the county is closed. The most exposed county is the island of Gotland, followed by Uppsala and Stockholm, adjacent to each other. The fact that these latter two counties are so highly exposed may be surprising, since the road networks in these counties are relatively dense. However, the travel demand in these counties is quite concentrated to the central city giving name to its respective county. This means that an area-covering event affecting this population center will make a large fraction of the trips in the county impossible. The analysis confirms that the most important cell for each county is indeed centered on central Stockholm and Uppsala, respectively. In Uppsala, 59.0 % of the trips cannot be made during the closure; the same shares for Stockholm and Gotland are 56.0 % and 63.4 %, respectively. This

unsatisfied demand constitutes 98.6 % of the total increase in travel time for Stockholm, 99.9 % for Uppsala and 99.97 % for Gotland.

We have also compared the worst-case user exposure for the 12.5 km grids with the worst-case user exposure for a single link failure. Figure 9 shows how many times worse the area-covering event would be to the county compared to the single link event. The figure shows that this ratio is the highest in densely populated areas. This is intuitively reasonable since high population density is strongly correlated with high road density, which makes the impacts of single link failures small (see Jenelius 2008a). More detailed analysis shows that in twelve of the 21 counties, the most important link is located within the most important cell. In some other cases, the two are located quite far from each other.

5. Conclusion and discussion

We have presented a method to analyse the vulnerability of road networks under area-covering disruptions. Since various kinds of real-world events such as snow storms and floods can cause such spatially extended disruptions, the analysis method is an important complement to the existing studies of single link failures. The approach is based on covering the study area with grids of equally shaped and sized cells, where each cell represents the extent of a disrupting event.

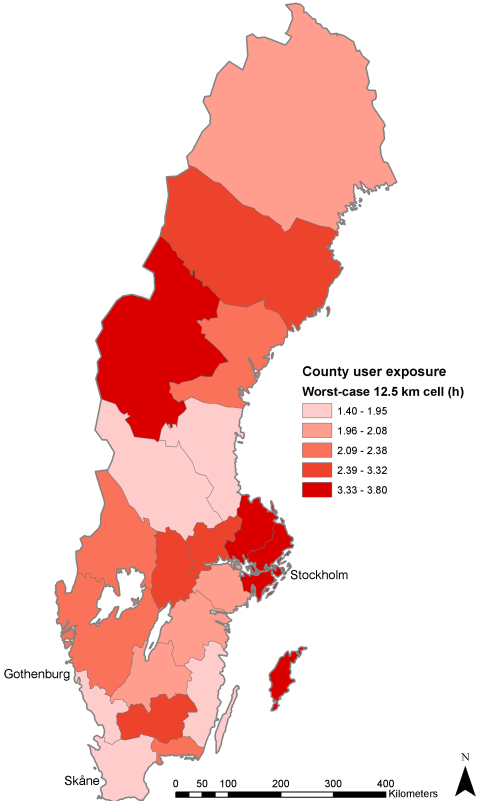


Fig. 8: Worst-case county user exposure for 12.5 km grids.

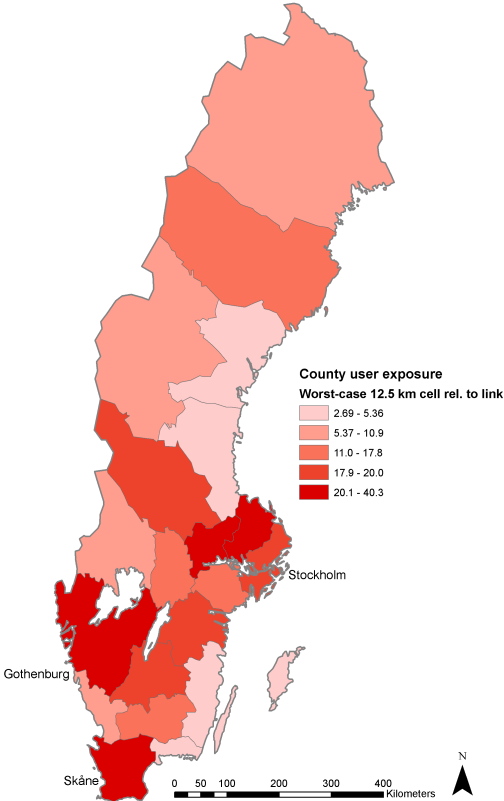


Fig 9. Worst-case county user exposure for 12.5 km grids relative to single links.

The application to the Swedish network shows that the factors determining where a spatially extended disruption will have the worst consequences are quite different from those of a single link failure. In the latter case, the flow on the link and the availability of alternative routes, i.e. the redundancy in the network, determines the consequences. For area-covering disruptions, the network redundancy has a much smaller impact, since nearby potential alternative links are often also disabled. It is the travel demand within, into and out from the affected area that largely determines the magnitude of the consequences. The unsatisfied demand, i.e. the trips that cannot be made during the closure, constitutes nearly all of the increase in travel time. Travel demand, in turn, is closely correlated with population size, which makes regions with the population concentrated to a few central locations particularly exposed to this kind of events.

The measure of regional exposure to an area-covering disruption is quite sensitive to how the regions are defined. First, there is a bias towards small regions being more exposed than large regions. This is because a disruptive event covers a larger fraction of a small region than a large, causing more severe consequences per user. Second, depending on how the regional borders are drawn, a certain population center may fall just within or just outside a particular region, which could have a large impact on the mean consequences for the region. To reduce these problems we presented exposure at the level of counties rather than for example the smaller municipalities, at which level the size bias is evident. Furthermore, the county borders have a clear economic and political role, which should make comparisons between different counties relevant.

References

- Beser, M. and Algiers, S. (2001) SAMPERS - The new Swedish national travel demand forecasting tool. In Lundqvist, L. and Mattsson, L.-G. (eds), *National Transport Models: Recent Developments and Prospects*, Advances in Spatial Science. Springer, 101-118.
- Buriol, L.S., Resende, M. G. C., Thorup, M., (2004) Speeding up dynamic shortest path algorithms. AT&T Labs Technical Report TD-5RJ8B. September 2003, revised August 2004.
- Chen, A., Yang, C., Kongsomsaksakul, S. and Lee, M. (2007) Network-based accessibility measures for vulnerability analysis of degradable transportation networks. *Networks and Spatial Economics* 7, 241–256.
- Jenelius, E. (2008a) Network structure and travel patterns: Explaining the geographical disparities of road network vulnerability, *Journal of Transport Geography*, in press.
- Jenelius, E. (2008b) Considering the user inequity of road network vulnerability, *Journal of Transport and Land Use*, accepted for publication.
- Jenelius, E., Petersen, T. and Mattsson, L.-G. (2006) Importance and exposure in road network vulnerability analysis. *Transportation Research Part A* 40, 537–560.
- Murray-Tuite, P. M. and Mahmassani, H. S. (2004) Methodology for determining vulnerable links in a transportation network, *Transportation Research Record* No. 1882, 88-96.

- Qiang, Q. and Nagurney, A. (2008) A unified network performance measure with importance identification and the ranking of network components. *Optimization Letters* 2, 127-142.
- Scott, D. M., Novak, D. C., Aultman-Hall, L. and Guo, F. (2006) Network Robustness Index: A new method for identifying critical links and evaluating the performance of transportation networks. *Journal of Transport Geography* 14, 215–227.
- Sohn, J. (2006) Evaluating the significance of highway network links under the flood damage: An accessibility approach. *Transportation Research Part A* 40, 491–506.
- Taylor, M. A. P., Sehkar, S. V. C. and D'Este, G. M. (2006) Application of accessibility based methods for vulnerability analysis of strategic road networks. *Networks and Spatial Economics* 6, 267–291.
- Zhan, F.B. and Noon, C.E. (1998) Shortest path algorithms: an evaluation using real road networks. *Transportation Science* 32, 65–73.